Hindawi
International Journal of RF and Microwave Computer-Aided Engineering
Volume 2023, Article ID 2311010, 8 pages
https://doi.org/10.1155/2023/2311010

Research Article

Generalized Complex-to-Complex Impedance Transformers Based on Conjugately Characteristic-Impedance Transmission Lines

Thanatcha Satitchantrakul,[1] **Akkarat Boonpoonga**,[2] **and Danai Torrungrueng**[3]

[1]*Department of Electronics Engineering Technology College of Industrial Technology, King Mongkut's University of Technology North Bangkok, Bangkok 10800, Thailand*
[2]*Research Center of Innovation Digital and Electromagnetic Technology, Faculty of Engineering, King Mongkut's University of Technology North Bangkok, Bangkok 10800, Thailand*
[3]*Research Center of Innovation Digital and Electromagnetic Technology, Department of Teacher Training in Electrical Engineering, Faculty of Technical Education, King Mongkut's University of Technology North Bangkok, Bangkok 10800, Thailand*

Correspondence should be addressed to Danai Torrungrueng; dtg@ieee.org

Received 12 November 2022; Revised 3 June 2023; Accepted 15 June 2023; Published 26 June 2023

Academic Editor: Giovanni Crupi

The novel technique of generalizing complex-to-complex impedance transformers (CCITs) with miniaturization is introduced in this paper. The generalized CCITs are designed based on conjugately characteristic-impedance transmission lines (CCITLs) along with the Meta-Smith charts (MSCs), resulting in convenient design equations. For illustration, a prototype of generalized CCITs is designed, simulated, and implemented with an asymmetric compact microstrip resonant cell (ACMRC), which is one of the CCITLs. The measurement results confirm that the proposed technique offers approximately 28.5% shorter in physical length compared to the CCIT designed using standard transmission lines.

1. Introduction

One of the fundamental radio-frequency modules of modern electronic devices is an impedance matching network (IMN) [1–3]. The simplest matching transformer is in the form of resistance-to-resistance transformers, i.e., quarter-wave transformers (QWTs). But the most general form is the complex impedance-matching transformer. Complex-to-complex impedance transformers (CCITs) are appeared in several papers [4–7], which can be implemented using transmission lines (TLs). In practice, TLs can be designed to be either symmetric, such as coplanar waveguide TLs and compact microstrip resonant cells (CMRCs) [8], or asymmetric such as asymmetric CMRCs (ACMRCs).

This paper proposes an alternative mathematical model of a generalized CCIT based on conjugate characteristic-impedance transmission lines (CCITLs) to achieve significant size reduction. Note that CCITLs have been introduced since 2004 [9–11]. In [9], the basic theory of CCITLs and the Meta-Smith charts (MSCs) were proposed, including their potential applications. In [10], quarter-wave-like transformers (QWLTs) based on CCITLs were successfully applied for miniaturized resistance-to-resistance transformers. Recently, a novel reactance-to-reactance transformer (RRT) based on CCITLs and MSCs has been proposed for size reduction [11].

In this paper, QWLTs and RRTs based on CCITLs are generalized for CCITs. It is found that the newly proposed CCIT can be designed using the MSCs and implemented using an ACMRC, where the CST Microwave Studio [12] is employed for simulations. After comprehensive review [13–18], the CCITs can be implemented using six approaches as follows: only one TL section, one TL and stubs, two TLs and stubs, three TLs and stubs, several TLs, and coupled TLs. As pointed out in [18], these methods cannot treat all possible complex termination impedances due to the lack of an available systematic design method, including unnecessarily complicated designs.

Among the six approaches, the CCITs implemented with a single TL on each transformer are recommended due to their useful, simple, reliable, diverse applications and the possible implementation of all other conventional designs [18]. Thus, this paper is considered only one TL section implemented with an ACMRC.

The originality and benefit of the proposed CCIT technique are to generalize CCITs implemented with a single standard TL to overcome some limitations. When both standard TL and CCITL can be employed to implement CCITs using only one TL section for specific input and output impedances, it can be shown that the CCIT implemented using the CCITL can offer shorter in both physical and electrical lengths compared to those of the CCIT implemented using the standard TL. In addition, the former can provide a wider range of input and output impedances for complex impedance matching compared to that of the single standard TL method.

The rest of this paper is organized as follows. Section 2 illustrates the theory of conventional CCITs and proposed CCITs. Both simulated and measured results are demonstrated in Section 3, including discussions. Finally, conclusions are presented in Section 4.

2. Theoretical Background

2.1. CCITS Implemented Using a Standard TL. A CCIT implemented using a standard TL is shown in Figure 1(a). A standard TL of length l, possessing the characteristic impedance (Z_0), propagation constant (β), and electrical length (θ), is employed to match between a complex output impedance ($Z_L = R_L + jX_L$) and a complex input impedance ($Z_{\text{in}} = R_{\text{in}} + jX_{\text{in}}$), where $\theta = \beta l$. In Figure 1(a), the output (Γ_{L}) and input (Γ_{in}) reflection coefficients can be expressed as [11].

$$\Gamma_L = \frac{R_L + jX_L - Z_0}{R_L + jX_L + Z_0}, \tag{1}$$

$$\Gamma_{\text{in}} = \frac{R_{\text{in}} + jX_{\text{in}} - Z_0}{R_{\text{in}} + jX_{\text{in}} + Z_0}. \tag{2}$$

The complex impedance matching problem can be easily designed with the Smith chart, as shown in Figure 2. Figures 2(a) and 2(b) illustrate the Smith chart for the cases of $\theta_{\text{in}} < \theta_L$ and $\theta_{\text{in}} > \theta_L$, respectively. Note that z_L and z_{in} in Figure 2 are the normalized Z_L and Z_{in} with respect to Z_0, respectively. In addition, θ_{in} and θ_L in Figure 2 are the angles associated with z_{in} and z_L in the complex reflection coefficient plane, respectively.

In the case of $\theta_{\text{in}} < \theta_L$, Γ_{L}, and Γ_{in} are related to the phase relationship as [11]

$$\frac{R_L + jX_L - Z_0}{R_L + jX_L + Z_0} = e^{j2\theta}\frac{R_{\text{in}} + jX_{\text{in}} - Z_0}{R_{\text{in}} + jX_{\text{in}} + Z_0}, \tag{3}$$

where Equations (1) and (2) are employed to obtain Equation (3). Similarly, Γ_L and Γ_{in} are related to the phase relationship in the case of $\theta_{\text{in}} > \theta_L$ as [11]

$$\frac{R_{\text{in}} + jX_{\text{in}} - Z_0}{R_{\text{in}} + jX_{\text{in}} + Z_0} = e^{j2(\pi-\theta)}\frac{R_L + jX_L - Z_0}{R_L + jX_L + Z_0}. \tag{4}$$

It is obvious that Equations (3) and (4) are identical to each other. After rearranging Equation (3), Z_0 of the CCIT can be found as

$$Z_0 = \sqrt{\frac{|Z_{\text{in}}|^2 R_L - |Z_L|^2 R_{\text{in}}}{R_{\text{in}} - R_L}}. \tag{5}$$

Note that Z_0 is independent of θ. In Equation (5), Z_0 exists if the following condition is satisfied:

$$\frac{|Z_{\text{in}}|^2 R_L - |Z_L|^2 R_{\text{in}}}{R_{\text{in}} - R_L} > 0. \tag{6}$$

However, it is implied from Equation (6) that this CCIT cannot match an arbitrary Z_{in} to an arbitrary Z_L in all cases. Once Z_0 is known, θ of the CCIT can be obtained as

$$\theta = \tan^{-1}\left(\frac{|z_{\text{in}}|^2 x_L - |z_L|^2 x_{\text{in}} + x_{\text{in}} - x_L}{|z_{\text{in}} z_L - 1|^2}\right), \tag{7}$$

where x_L and x_{in} are the normalized X_L and X_{in} with respect to Z_0, respectively.

2.2. Generalized CCITS Implemented Using a CCITL. The CCIT implemented using a CCITL is shown in Figure 1(b) to match between a complex output impedance Z_L to a complex input impedance Z_{in}, where $Z_c^{\pm}$, β_c and θ_c are the characteristic impedances, propagation constant, and electrical length of the CCITL, respectively. Note that $Z_c^{\pm}$ can be expressed as [11]

$$Z_c^{\pm} = \left|Z_c^{\pm}\right| e^{\mp j\phi}, \tag{8}$$

where $|Z_c^{\pm}|$ is the absolute value of $Z_c^{\pm}$ and ϕ is the argument of Z_c^{-}. Note that ϕ is set in the range of $-90\circ \leq \phi \leq 90\circ$. In Figure 1(b), Γ_L and Γ_{in} represent the load and input reflection coefficients for the CCITL, respectively, which can be expressed as [9]

$$\Gamma_L = \frac{Z_L Z_c^{-} - |Z_c^{\pm}|^2}{Z_L Z_c^{+} + |Z_c^{\pm}|^2}, \tag{9}$$

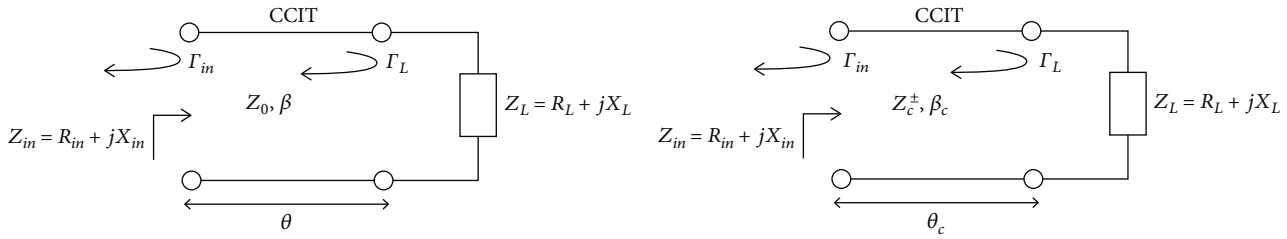

FIGURE 1: A CCIT implemented using (a) a standard TL and (b) a CCITL.

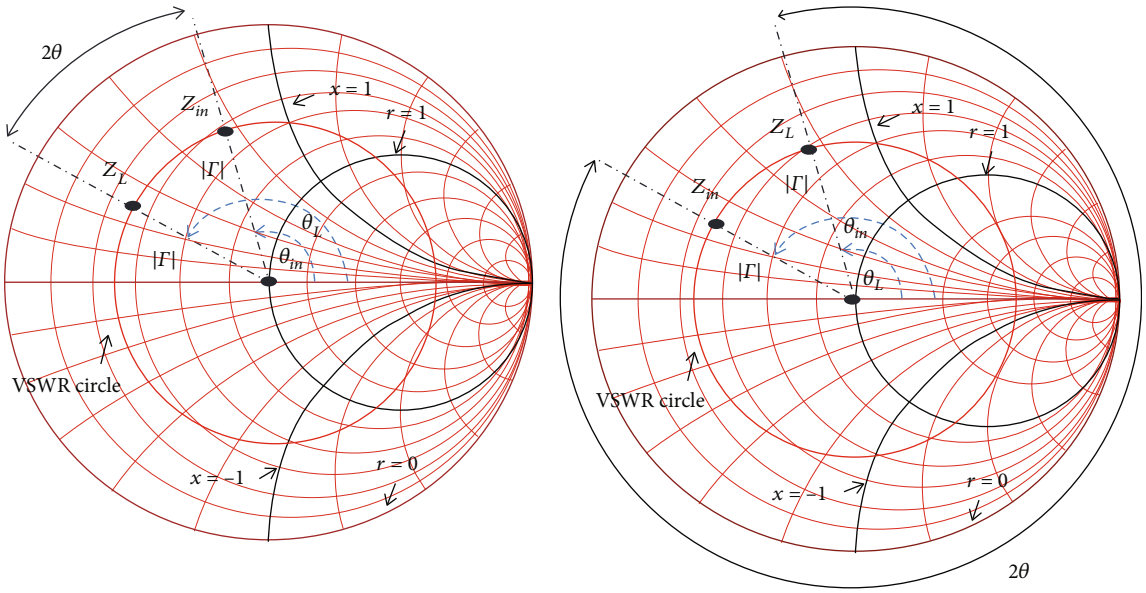

FIGURE 2: The Smith chart calculation of a CCIT using a standard TL. (a) $\theta_{in} < \theta_L$. (b) $\theta_{in} > \theta_L$.

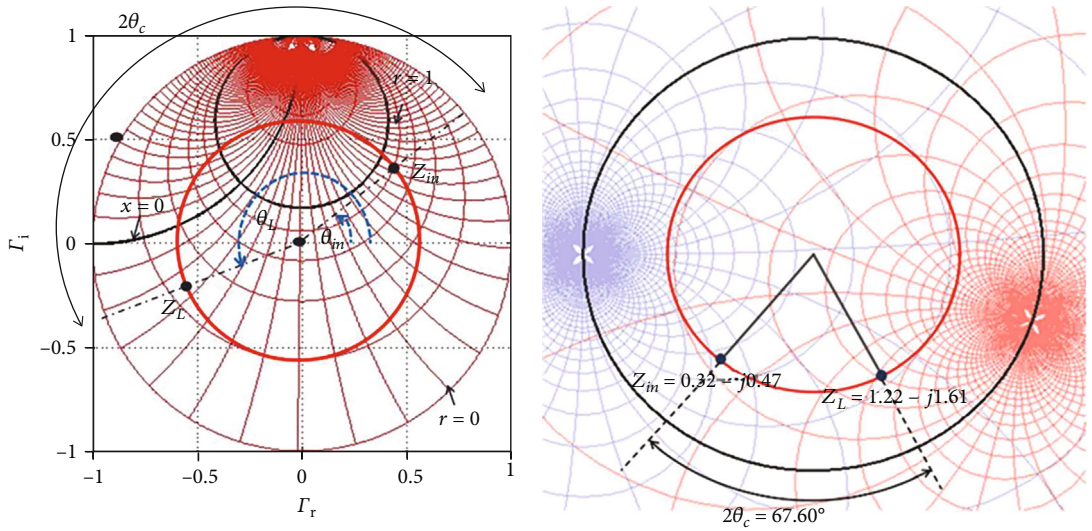

FIGURE 3: (a) The MSC ($\phi = 45\circ$) for case 1 with and $0\circ \leq \theta c \leq 180\circ$. (b) The MSC ($\phi = -9.02\circ$) for case 4 with $\theta c = 33.80\circ$.

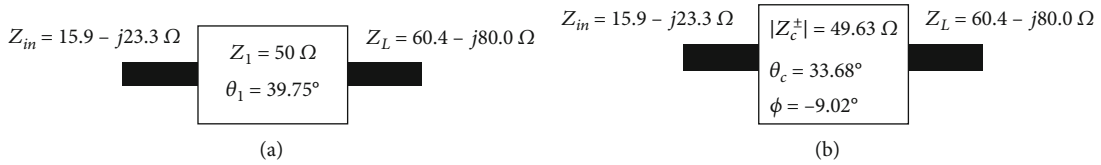

FIGURE 4: Complex-to-complex impedance transformers (CCITs) using (a) a standard TL and (b) a CCITL based on an ACMRC.

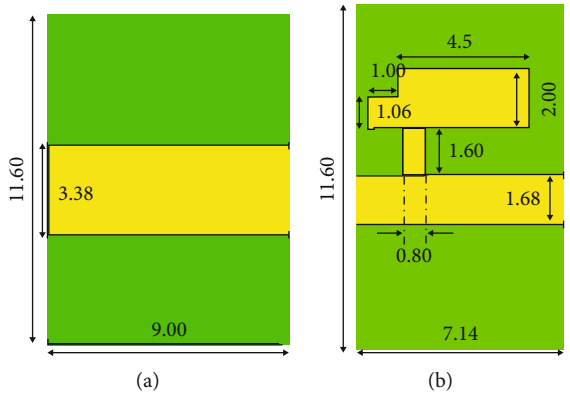

FIGURE 5: Schematic design using the CCIT (dimension in mm) implemented using (a) a standard TL and (b) a CCITL based on an ACMRC.

$$\Gamma_{\text{in}} = \frac{Z_{\text{in}}Z_c^- - |Z_c^{\pm}|^2}{Z_{\text{in}}Z_c^+ + |Z_c^{\pm}|^2}. \tag{10}$$

In [9], the MSCs are employed to design the stub tuners and periodic TL structures. In this work, the MSCs are applied to design CCITs implemented using CCITLs. From the MSC viewpoint, there are 4 cases to consider as follows [11]:

Case 1: $\theta_{\text{in}} < \theta_L$ and $0^\circ \le \phi \le 90^\circ$ (see Figure 3(a))

Case 2: $\theta_{\text{in}} < \theta_L$ and $-90^\circ \le \phi \le 0^\circ$

Case 3: $\theta_{\text{in}} > \theta_L$ and $0^\circ \le \phi \le 90^\circ$

Case 4: $\theta_{\text{in}} > \theta_L$ and $-90^\circ \le \phi \le 0^\circ$

In Figure 3(a), z_L and z_{in} are the normalized Z_L and Z_{in} with respect to $|Z_c^{\pm}|$, respectively. Note that Γ_r and Γ_i are real and imaginary parts of Γ, respectively. Similar to the cases of the Smith chart in Section 2.1, Γ_L and Γ_{in} in all cases of MSCs above are also related via the phase relationship. For case 1, Equations (8)–(10) can be readily rearranged as [11].

$$\frac{Z_L e^{j\phi} - |Z_c^{\pm}|}{Z_L e^{-j\phi} + |Z_c^{\pm}|} = e^{j2\theta_c} \frac{Z_{\text{in}} e^{j\phi} - |Z_c^{\pm}|}{Z_{\text{in}} e^{-j\phi} + |Z_c^{\pm}|}. \tag{11}$$

After rearranging Equation (11) by considering only the magnitude for both sides of Equation (11), $|Z_c^{\pm}|$ can be determined straightforwardly as

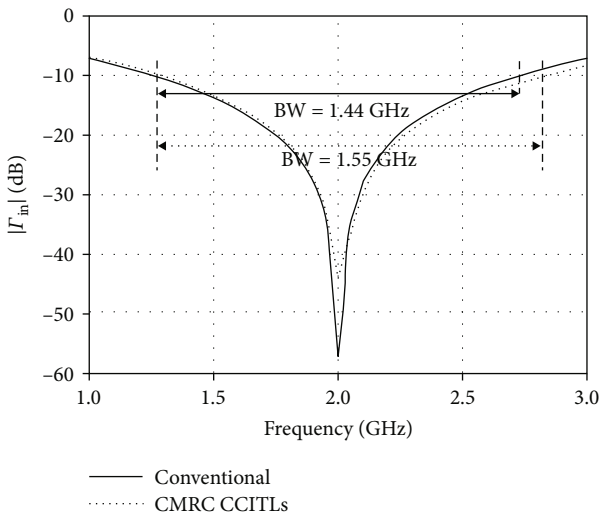

FIGURE 6: Plot of simulated bandwidths of the CCITs implemented using a standard TL and a CCITL based on an ACMRC.

$$|Z_c^{\pm}| = \frac{(R_L X_{\text{in}} - R_{\text{in}} X_L)\sin\phi}{(R_{\text{in}} - R_L)} \frac{\pm\sqrt{(R_L X_{\text{in}} - R_{\text{in}} X_L)^2 \sin^2\phi - (R_{\text{in}} - R_L)\left(|Z_L|^2 R_{\text{in}} - |Z_{\text{in}}|^2 R_L\right)}}{(R_{\text{in}} - R_L)}. \tag{12}$$

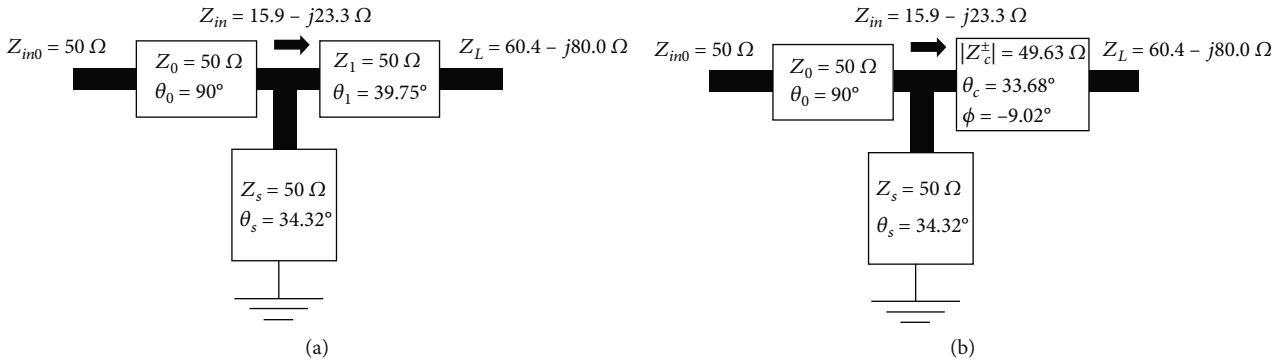

FIGURE 7: Shunt stub tuning circuit using the CCIT implemented using:(a) a standard TL and (b) a CCITL.

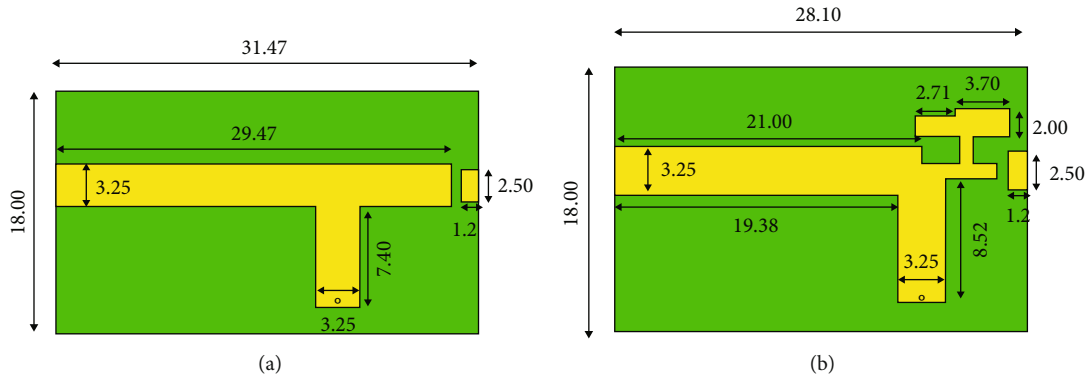

FIGURE 8: Schematic design of the shunt stub tuning circuit using the CCIT (dimension in mm) implemented using (a) a standard TL and (b) a CCITL based on an ACMRC.

Note that $|Z_c^{\pm}|$ depends on ϕ but is independent of θ_c. In addition, when $\phi = 0\circ$ (corresponding to the standard TL method), Equation (12) is reduced to Equation (5) as expected. Once $|Z_c^{\pm}|$ is known via Equation (12), θ_c of the CCIT implemented using a CCITL can be expressed as

$$\theta_c = \tan^{-1}\left(\frac{\Gamma_{\text{in},L}\cos\phi}{\sin\phi + j\left(|Z_c^{\pm}|^2 - Z_{\text{in}}Z_L/|Z_c^{\pm}|(Z_{\text{in}}+Z_L)\right)}\right), \tag{13}$$

where

$$\Gamma_{\text{in},L} = \frac{Z_{\text{in}} - Z_L}{Z_{\text{in}} + Z_L}. \tag{14}$$

Thus, Equations (12) and (13) are the design equations for the CCIT implemented using a CCITL. Note that Equation (12) requires that the term inside the square root, and $|Z_c^{\pm}|$ must be nonnegative; i.e., the following conditions are satisfied:

$$(R_L X_{\text{in}} - R_{\text{in}} X_L)^2 \sin^2\phi - (R_{\text{in}} - R_L)\left(|Z_L|^2 R_{\text{in}} - |Z_{\text{in}}|^2 R_L\right) > 0, \tag{15}$$

$$\frac{(R_L X_{\text{in}} - R_{\text{in}} X_L)\sin\phi \pm \sqrt{(R_L X_{\text{in}} - R_{\text{in}} X_L)^2 \sin^2\phi - (R_{\text{in}} - R_L)\left(|Z_L|^2 R_{\text{in}} - |Z_{\text{in}}|^2 R_L\right)}}{(R_{\text{in}} - R_L)} > 0. \tag{16}$$

It should be pointed out that, when $\phi = 0\circ$, Equations (15) and (16) are reduced to Equation (6) as expected. Note that Equations (15) and (16) depend on ϕ, providing another degree of freedom and possibly leading to a wider range of Z_L and Z_{in} for complex impedance matching, compared to that of the standard TL method. For CCITs implemented using only one TL section, there is a forbidden region in the impedance domain, defined as an area where one TL cannot transform a complex impedance into another one [18–20]. Thus, the CCIT implemented using a CCITL can

Table 1: Comparison between the CCITs implemented using a standard TL and a CCITL based on an ACMRC.

	CCIT using a standard TL (1st CCIT)	CCIT using a CCITL based on an ACMRC (2nd CCIT)	The modified 1st CCIT as a part of shunt tuning stub	The modified 2nd CCIT as a part of shunt tuning stub
Electrical length (degree)	39.75	33.68	—	—
Physical length (mm)	9.00	7.14	6.84	6.4
Bandwidth (GHz)	1.45	1.55	—	—

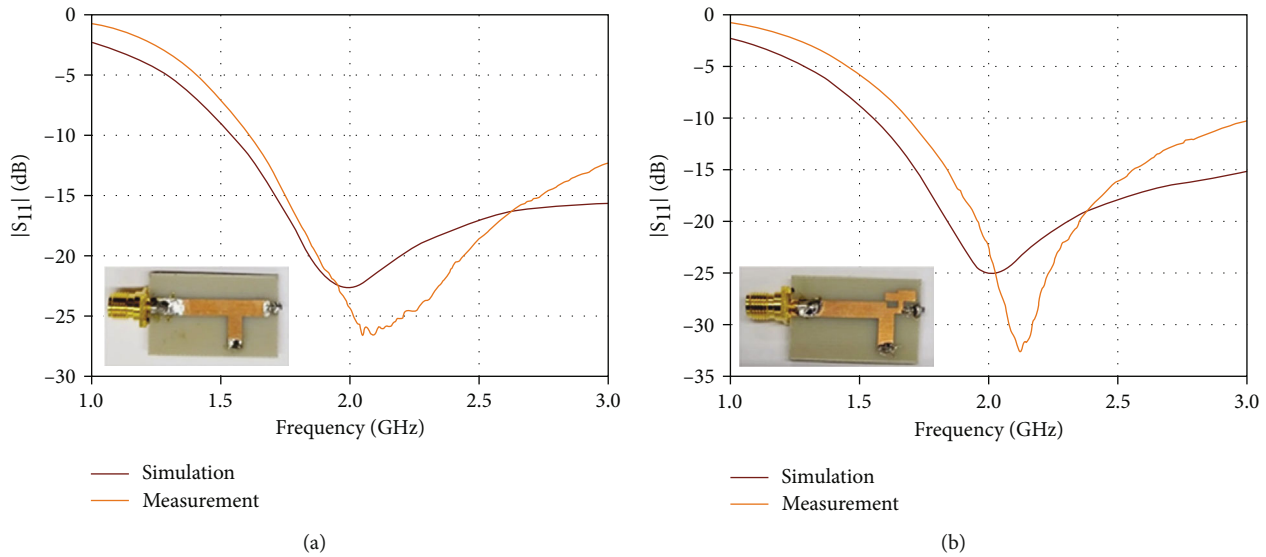

Figure 9: Plots of the simulated and measured $|S_{11}|$ of the shunt stub tuning circuit using the CCIT implemented using (a) a standard TL and (b) a CCITL based on an ACMRC.

possibly reduce the forbidden region due to the reason explained above. However, similar to the CCIT in Section 2.1, this CCIT may not match an arbitrary Z_{in} to an arbitrary Z_L in all cases.

For cases 2 to 4, it is found that the CCIT design equations are still Equations (12) and (13). Note that the standard TL and the Smith Chart can be considered the special case of CCITLs and MSCs when $\phi = 0^\circ$ [9]. As expected, it can be shown that Equations (12) and (13) are reduced to Equations (5) and (7), respectively.

3. Results and Discussions

For illustration, the CCIT implemented using a CCITL is designed to match a complex output impedance $Z_L = 60.4 - j80\,\Omega$ to a complex input impedance $Z_{\text{in}} = 15.9 - j23.3\,\Omega$. In this case, ϕ is assumed to be -9.02°. Using Equation (12), $|Z_c^{\pm}|$ is found to be 49.63 Ω. Figure 3(b) illustrates the MSC design for normalized Z_{in} and Z_L, corresponding to case 4. It is found from the MSC when $\phi = -9.02^\circ$ that $\Gamma_{\text{L}} = 0.30 - j0.56$, $\Gamma_{\text{in}} = -0.41 - j0.49$, and $\theta c = 33.80^\circ$, which are almost identical to the design parameters from Equations (9) and (10) ($\Gamma_L = 0.29 - j0.56$ and $\Gamma_{\text{in}} = -0.40 - j0.49$) and Equation (13) ($\theta c = 33.68^\circ$) as expected.

The schematic diagrams of the CCITs are shown in Figures 4(a) and 4(b) for the CCIT implemented using a standard TL and a CCITL based on an ACMRC, respectively. For this load Z_L, the resistor of 60.4 Ω and capacitor of 1 pF are connected in series to obtain $Z_L = 60.4 - j80\,\Omega$ at the operating frequency of 2 GHz. For the CCIT implemented using a standard TL (called the 1st CCIT), Equations (5) and (7) are employed to determine Z_1 and θ_1 in Figure 4(a), respectively. It is found that $Z_1 = 50\,\Omega$ and $\theta_1 = 39.75^\circ$. For the CCIT implemented using a CCITL (called the 2nd CCIT), Equations (12) and (13) are employed to determine $|Z_c^{\pm}|$ and θ_c in Figure 4(b), respectively. For a given $\phi = -9.02^\circ$, it is found that $|Z_c^{\pm}| = 49.63\,\Omega$ and $\theta_c = 33.68^\circ$. To implement both CCITs, the CST Microwave Studio is employed to simulate desired microstrip structures on the FR-4 substrate (dielectric constant of 4.3, loss tangent of 0.02, and substrate thickness of 1.6 mm), as illustrated in Figure 5, where their dimension is given in mm. It is clearly seen that the CCITL approach offers approximately 100 MHz wider bandwidth, as shown in Figure 6, with a 20% shorter in physical length compared to that of the standard TL approach. Note that the input reflection coefficient Γ_{in} in Figure 6 is defined as

$$\Gamma_{\text{in}} = \frac{Z_{\text{in}} - Z_{\text{in,ref}}}{Z_{\text{in}} + Z_{\text{in,ref}}}, \tag{17}$$

where Z_{in} is the input impedance of the considered CCIT and $Z_{\text{in,ref}}$ is the desired input impedance of the CCIT

Table 2: Comparison between the CCITs implemented using a standard TL in [20] and a CCITL using $\phi = -45^\circ$ for $Z_L = 120 - j30\,\Omega$ and $Z_{in} = R_{in} - j40\,\Omega$.

R_{in} (Ω)	Z_0 (Ω)	θ ($^\circ$)	$\lvert Z_c^{\pm}\rvert$ (Ω)	θ_c ($^\circ$)
20	25.69	25.44	9.57	6.09
40	53.39	35.44	30.33	10.31
60	70.00	32.47	43.07	8.60
80	81.24	24.29	49.23	5.62
100	83.07	12.02	41.00	2.34

design at the operating frequency of 2 GHz, which is equal to 15.9-j23.3 Ω in this case.

Finally, the CCITs are integrated with the shunt stub tuning circuit operating at 2 GHz, as shown in Figure 7, for both standard TL and CCITL implementations. The CST Microwave Studio will also be used to appropriately adjust the formerly designed microstrip structures of both CCIT implementations (called the modified 1st and 2nd CCITs) due to coupling effects after integrating the CCITs into the shunt stub tuning circuit. The optimized designs are presented with dimensions in Figures 8(a) and 8(b) for the CCITs using a standard TL and a CCITL implemented by an ACMRC, respectively. In addition, the insertions in Figures 8(a) and 8(b) illustrate CCIT prototypes implemented using a standard TL and a CCITL implemented by an ACMRC, respectively. Note that the proposed design offers approximately 28% shorter in physical length compared to that of the CCIT implemented using a standard TL. Furthermore, the comparison between the CCITs implemented using a standard TL and a CCITL based on an ACMRC in terms of electrical length, physical length, and bandwidth is summarized in Table 1 for clarity.

Figure 9 also illustrates the plots of the magnitude of the input reflection coefficient ($\lvert S_{11}\rvert$) for both simulation and measurement of both CCITs implemented using a standard TL and a CCITL based on an ACMRC. It is clearly seen that the measurement results offer better $\lvert S_{11}\rvert$ at -27.5 dB and -34.3 dB compared to the simulation results at -22 dB and -25 dB of the CCIT implemented using the standard TL and the CCITL, respectively. However, the measurement results also show a slightly shifted operating frequency from 2 GHz to 2.1 GHz and 2.2 GHz for the CCITs implemented using the standard TL and the CCITL, respectively.

In addition, Table 2 illustrates the comparison between the CCITs implemented using a standard TL in [20] and a CCITL using $\phi = -45^\circ$ for $Z_L = 120 - j30\,\Omega$ and $Z_{in} = R_{in} - j40\,\Omega$, where five values of R_{in} are considered and the TL parameters are given for both the standard TL and the CCITL for each R_{in}. From Table 2, it is found that, for specific Z_L and Z_{in}, the CCIT implemented using the CCITL can offer significantly shorter electrical lengths compared to those of the CCIT implemented using the standard TL.

4. Conclusions

The generalized CCITs implemented using a CCITL based on an ACMRC are proposed in this paper, where they are systematically designed using the MSCs, resulting in convenient design equations. It is shown that the proposed method can miniaturize both the physical and electrical sizes of desired CCITs. In addition, the simulated and measured results confirm that the CCIT implemented using the CCITL can indeed offer shorter in both physical and electrical lengths, compared to those of the CCIT implemented using the standard TL. Furthermore, the CCIT implemented using a CCITL can possibly reduce the forbidden region, compared to that of the CCIT implemented using a single standard TL due to an extra degree-of-freedom parameter ϕ of the CCITL model.

Data Availability

Data sharing not applicable to this article as no datasets were generated or analyzed during the current study.

Conflicts of Interest

The authors declare that they have no conflicts of interest.

Acknowledgments

This research was funded by the King Mongkut's University of Technology North Bangkok, contract no. KMUTNB-65-KNOW-12.

References

[1] D. M. Pozar, *Microwave Engineering*, John Wiley & Sons, Hoboken, NJ, 2012.

[2] R. K. Maharajan and N. Y. Kim, "Miniature stubs-loaded square open-loop bandpass filter with asymmetrical feeders," *Microwave and Optical Technology Letters*, vol. 55, no. 2, pp. 329–332, 2012.

[3] I. Sakagami, M. Haga, and T. Munehiro, "Reduced branch-line coupler using eight two-step stubs," *IEE Proceedings-Microwaves, Antennas and Propagation*, vol. 146, no. 6, pp. 455–460, 1999.

[4] C. Füzy and A. Zólomy, "Design of broadband complex impedance-matching networks and their applications for broadbanding microwave amplifiers," in *Proceedings of the 18-Th International Conference on Microwaves, Radar and Wireless Communications*, Vilnius, Lithuania, 2010.

[5] H.-R. Ahn and S. Nam, "3-dB power dividers with equal complex termination impedances and design methods for controlling isolation circuits," *IEEE Transactions on Microwave Theory and Techniques*, vol. 61, no. 11, pp. 3872–3883, 2013.

[6] Q. Gu, J. R. Luis, A. S. Morris, and J. Hilbert, "An analytical algorithm for Pi-network impedance tuners," *IEEE Transactions on Circuits and Systems I: Regular Papers*, vol. 58, no. 12, pp. 2894–2905, 2011.

[7] R. Sinha and A. De, "Theory on matching network in viewpoint of transmission phase shift," *IEEE Transactions on Microwave Theory and Techniques*, vol. 64, no. 6, pp. 1704–1716, 2016.

[8] P. Kurgan, J. Filipcewicz, and M. Kitlinski, "Development of a compact microstrip resonant cell aimed at efficient microwave component size reduction," *IET Microwaves, Antennas & Propagation*, vol. 6, no. 12, pp. 1291–1298, 2012.

[9] D. Torrungrueng, *Meta-Smith Charts and their Potential Applications*, Morgan & Claypool, San Rafael, CA, 2010.

[10] T. Satitchantrakul, P. Akkaraekthalin, R. Silapunt, and D. Torrungrueng, "Compact wideband multi-section quarter-wave-like transformers," *Journal of Electromagnetic Waves and Applications*, vol. 32, no. 15, pp. 1911–1924, 2018.

[11] T. Satitchantrakul and D. Torrungrueng, "Design of reactance-to-reactance impedance transformers based on conjugately characteristic impedance transmission lines (CCITLs) and meta-smith charts (MSCs)," *Radioengineering*, vol. 30, no. 2, pp. 349–356, 2021.

[12] "CST microwave studio," 2019, http://www.cst.com.

[13] H. Jasik, *Antenna engineering handbook*, McGraw-Hill, New York, 1st edition, 1961.

[14] T. A. Milligan, "Transmission-line transformation between arbitrary impedances (letters)," *IEEE Transactions on Microwave Theory and Techniques*, vol. 24, no. 3, p. 159, 1976.

[15] M. H. N. Potok, "Comments on "transmission-line transformation between arbitrary impedances"," *IEEE Transactions on Microwave Theory and Techniques*, vol. 25, no. 1, p. 77, 1977.

[16] S. J. Orfanidis, *Electromagnetic Waves and Antennas*, Department of Electrical and Computer Engineering, Rutgers University, Piscataway, NJ, 2016.

[17] H.-R. Ahn, *Asymmetric Passive Components in Microwave Integrated Circuits*, Wiley, Hoboken, NJ, 2006.

[18] H.-R. Ahn and M. M. Tentzeris, "Complex impedance transformers: their use in designing various ultracompact and wideband power dividers," *IEEE Microwave Magazine*, vol. 21, no. 9, pp. 53–64, 2020.

[19] H.-R. Ahn and M. M. Tentzeris, "Complex impedance transformers based on allowed and forbidden regions," *IEEE Access*, vol. 7, pp. 39288–39298, 2019.

[20] H.-R. Ahn, "Complex impedance transformers consisting of only transmission-line sections," *IEEE Transactions on Microwave Theory and Techniques*, vol. 60, no. 7, pp. 2073–2084, 2012.